UCRL-17504

University of California

Ernest O. Lawrence Radiation Laboratory

INFLUENCE OF CORIOLIS COUPLING, PAIRING, AND OCTUPOLE VIBRATION-PARTICLE COUPLING ON $\Delta K = -1$ E1 TRANSITION IN ^{177}Hf

TWO-WEEK LOAN COPY

This is a Library Circulating Copy which may be borrowed for two weeks. For a personal retention copy, call Tech. Info. Division, Ext. 5545

Berkeley, California

DISCLAIMER

This document was prepared as an account of work sponsored by the United States Government. While this document is believed to contain correct information, neither the United States Government nor any agency thereof, nor the Regents of the University of California, nor any of their employees, makes any warranty, express or implied, or assumes any legal responsibility for the accuracy, completeness, or usefulness of any information, apparatus, product, or process disclosed, or represents that its use would not infringe privately owned rights. Reference herein to any specific commercial product, process, or service by its trade name, trademark, manufacturer, or otherwise, does not necessarily constitute or imply its endorsement, recommendation, or favoring by the United States Government or any agency thereof, or the Regents of the University of California. The views and opinions of authors expressed herein do not necessarily state or reflect those of the United States Government or any agency thereof or the Regents of the University of California.

Submitted to Nucl. Phys.

UCRL-17504
Preprint

UNIVERSITY OF CALIFORNIA

Lawrence Radiation Laboratory
Berkeley, California

AEC Contract No. W-7405-eng-48

INFLUENCE OF CORIOLIS COUPLING, PAIRING, AND OCTUPOLE VIBRATION-PARTICLE COUPLING ON $\Delta K = -1$ E1 TRANSITION IN ^{177}Hf

F. M. Bernthal and J. O. Rasmussen

April 1967

Influence of Coriolis coupling, pairing, and octupole vibration-particle coupling on $\Delta K = -1$ E1 transitions in ^{177}Hf*

F. M. Bernthal and J. O. Rasmussen

Lawrence Radiation Laboratory and Department of Chemistry
University of California
Berkeley, California

April 1967

Abstract: A fit of 14 $\Delta K = -1$ E1 transitions in ^{177}Hf to within 20% of experimentally derived absolute intensities was achieved by considering the principal and Coriolis-mixed E1 components as three adjustable parameters. Subsequent theoretical calculations using Nilsson wave functions and including the effects of pairing, Coriolis coupling, and octupole vibration-particle coupling yielded a fit to within a factor of two for the ^{177}Hf E1 intensities. Only one adjustable parameter, the octupole vibration-particle coupling strength, was used in the microscopic calculations. Three new transitions including two new E1's have been observed in the decay of $^{177}Lu^m$. Improved E1 relative intensity measurements are presented for comparison with theory.

E	RADIOACTIVITY $^{177}Lu^m$ [from ^{176}Lu (n,γ)]; measured E_γ, I_γ. ^{177}Hf deduced B(E1). Natural target.

*The work supported by the U. S. Atomic Energy Commission.

1. Introduction

The strong influence of Coriolis-admixed components on the $\Delta K = \pm 1$ electric dipole transitions in odd-mass deformed nuclei is now well recognized[1,2]. Several authors have considered the effects of Coriolis mixing in attempting to explain anomalies in experimentally observed branching ratios of E1 radiation. Although considerable success has been realized in predicting and accounting for E1 branching ratios that strongly violate Alaga's rules, relatively poor agreement with experiment has resulted from all attempts to explain quantitatively the absolute E1 transition strengths.

The 16 E1 transitions arising from the decay of 161-day[3] $^{177}Lu^{m}$ to high spin members in ^{177}Hf provide an exceptionally rigorous experimental test for theoretical study of $\Delta K = 1$ E1 transitions. As is typical for this class of E1 transition, the Nilsson hindrance factors $F_N = B_N(E1)/B_{exp}(E1)$ for the ^{177}Hf E1's vary from near unity in several cases to $\sim 10^3$ in the case of the well-known 321-keV transition between the 9/2 + [624] and 7/2 - [514] band heads. Such wide variation in E1 transition rates between the same intrinsic states cannot be explained in terms of simple transition rate theory.

It can now be shown that it is possible within the framework of the unified model to successfully account for the absolute E1 transition strengths in ^{177}Hf to a relatively small margin of error. The method used in the microscopic calculations involves consideration of Coriolis-mixed E1 components, pairing reduction, and collective E1 components arising from octupole vibration-particle coupling.* Improved experimental data for the ^{177}Hf E1's are presented for comparison with theory.

---

*We have recently received a copy of the thesis of R. Piepenbring (University of Strassburg) in which the influence of collective octupole components on $|\Delta K| = 1$ E1 transitions in odd-A deformed nuclei is discussed using a somewhat different approach from ours, but we have not had time to make a detailed comparison in this article.

2. Deduction of Experimental E1 Strengths in ^{177}Hf

Because of the wide variation in E1 strengths in ^{177}Hf, we have expended considerable effort in an attempt to obtain the best possible experimental measurements for the relative E1 intensities. Singles spectra of the decay of $^{177}Lu^m$ have been taken using the anti-Compton Ge(Li) spectrometer at Livermore (7 cm^3, resolution 1.1 keV at 122 keV) and a high resolution (0.77 keV at 122 keV) Ge(Li) crystal in our laboratory. In fig. 1 we display a portion of the $^{177}Lu^m$ gamma ray spectrum taken on the anti-Compton device. The favorable peak-to background ratio obtainable has enabled us to identify the 88.4-keV E1 transition between the spin 19/2 members of the two ^{177}Hf rotational bands. Moreover, the 242.5-keV M1-E2 cascade transition leading from the 21/2 to the 19/2 spin level of the K = 7/2 - band has also been observed with intensity (0.32 ± 0.4)% relative to the 105.4-keV line. Figures 2 and 3 show linear plots of the 88.4- and 242.5-keV photopeaks. The high-resolution spectra taken on the 1 cm^2 × 9 mm depletion depth "thin window" Ge(Li) crystal have facilitated the confirmation of the 69.2-keV E1 transition tentatively assigned earlier[4] and have allowed more accurate measurement of relative intensities for several previously reported E1's. In fig. 4 we show the linear plot of the 69.2-keV line. Figures 5 and 6 show two particularly interesting regions of the $^{177}Lu^m$ spectrum. The 117.2- and 145.8-keV E1's seen in ref. 4) as only poorly defined shoulders on the 116.0- and 147.2-keV lines are now resolved. The second partial spectrum shows that the very weak 283.4-keV E1 is nearly resolved from the 281.8-keV photopeak, and the E1 doublet at 292 keV now clearly shows the 292.5-keV line to be weaker than the 291.4-keV E1. In fig. 7 we display again for reference the now well established decay scheme of $^{177}Lu^m$. With the exception of the three transitions

added from the present work and the slightly altered half-life of $^{177}Lu^{m}$,[3] the scheme is exactly the same as reported and modified by earlier workers[4,5,6,7].

Table 1 shows the composite relative intensity data for the 14 E1 transitions observed to date. Also shown are the derived experimental values of B(E1). The lifetime of the 321-keV level has been measured by Berlovich, et al.[8] to be $\tau_{1/2} = (6.9 \pm 0.3) \times 10^{-10}$ sec. Using this value and the M2/E1 mixing ratio 0.18 for the 321-keV E1,[9] it is possible from relative intensity measurements to calculate directly the reduced strengths of the three E1's leading from the 9/2+[624] band head.

All other values of B(E1) have been derived using the rotational model of Bohr and Mottelson, assuming $Q_0 = 6.85$ barns[10]. For all E1's except those leading from the 11/2+ member of the K = 9/2+ band, crossover E2 intensities may be used to deduce B(E1) for transitions from a given level. For the E1's leading from the 11/2+ level, values of B(E1) were derived from the rotational M1-E2 transition strength of the 105.4-keV cascade γ ray taking $(1/\delta^2) = [T_\gamma'(M1)]/[T_\gamma'(E2)] = 8.7$ by extrapolation to spin 11/2 in fig. 8. In contrast to the similar analysis first performed for ^{177}Hf by Alexander et al.[5] which neglected the effects of Coriolis mixing in the 9/2+[624] band, we have now taken into account the contributions of Coriolis-mixed components to the intraband transition strengths. The wave amplitudes for the Coriolis-mixed components originating from the $i_{13/2}$ shell model state were obtained by Holtz in a matrix diagonalization. The procedure used reproduces the experimentally observed energy levels of the rather strongly perturbed ^{177}Hf 9/2+[624] band to within less than 0.4 keV by varying the effective size of the off-diagonal RPC matrix elements[11].

3. ^{177}Hf E1 Transition Strengths in the Unified Model

It has been shown by Grin and Pavlichenkov[1] and by Vergnes and Rasmussen[2] using analyses equivalent in their conclusions that a simple first order perturbation treatment which regards the principal and Coriolis-mixed ^{177}Hf E1 matrix elements as two adjustable parameters can explain quite successfully the observed E1 branching ratios. In fact, the more complete analysis in ref. 1) showed the general validity of this treatment in explaining the anomalous branching ratios of $|\Delta K| = 1$ E1's in odd-mass deformed nuclei. In fig. 9 we show the results of such a simple treatment applied to the ^{177}Hf E1 intensities from this work.

As indicated in ref. 1), the terms which should be considered up to first order in the analysis of the ^{177}Hf E1's are the following: 1) the principal 9/2+[624] → 7/2-[514] component; 2) the Coriolis-admixed (K=7/2+) → 7/2-[514] components; 3) the 9/2+[624] → (K=9/2-) Coriolis-admixed components. We have obtained an estimate of the wave-function coefficient for the Coriolis-mixed 7/2+[633] component in the 9/2+[624] band from the band-fit matrix diagonalization mentioned earlier. The mixing of K = 9/2- components into the 7/2-[514] band was estimated by a simple first-order perturbation treatment. Use of the normalized initial and final wave functions and treatment of the E1 matrix elements as three adjustable parameters yielded a fit to within 20% of the experimental absolute E1 transition strengths. Figures 10 and 11 show the normalized 3-parameter fit in comparison with the simple 2-parameter treatment and with experiment.

The quality of the fit thus obtained prompted an attempt to account for the observed absolute E1 strengths within the framework of the unified model.

Recent developments[12,13,14] in the theoretical interpretation of the collective octupole vibrational mode in deformed nuclei and its apparent application to the $\Delta K = 0$ class of E1 transitions[15,16] have suggested a similar important influence on $|\Delta K| = 1$ E1's, all of which apparently have relatively large $\Delta K = 0$ Coriolis-mixed components.

In our calculations we have followed the approach of Faessler et al.[16] who suggest the vibration-particle coupling Hamiltonian

$$H_{vp} = -\hbar \omega_0 a_{30} r^2 Y_{30}(\theta, \varphi)$$

which for $\Delta K = 0$ E1 transitions mixes the octupole band of the final state with the initial state and vice-versa. The only other quantities needed for the calculation are the octupole zero-point amplitude, $\langle a_3 \rangle = \hbar/\sqrt{2B_3E_3}$, and the collective E1 strength associated with the octupole vibration, $B_{coll}(E1)$. Experimental data on both B(E3) and B(E1) for transitions between the first octupole band (K=0-) and ground in even-even nuclei are extremely scarce in the rare-earth region. However, the recent publication of Donner and Greiner[13] offers estimates of the collective dipole and octupole strengths in this region. In this work, the E1 strength is derived by means of the Dynamic Collective Theory whereby E1 transitions of the octupole states are supposed to arise from small admixtures of giant dipole resonance. The pertinent relation given in ref. 13) is

$$\frac{B(E1)}{B_{sp}(E1)} = 5.74 \times 10^{-2} A C_0^2 (I_i 1 0 0 | I_f 0) \qquad (1)$$

where Co is the giant dipole wave function admixture coefficient for the $(K_i=0^- \rightarrow K_f=0^+)$, $|K_i-J_3|=0$ class of E1's.

Adopting the general approach suggested by Faessler et al.[16], and assuming $E_3=1.2$ MeV, we have calculated the reduced transition strengths in ^{177}Hf taking into account pairing reduction, the influence of the Coriolis RPC perturbation, and the second-order vibration-particle perturbation which mixes the initial and final states of the $\Delta K=0$ E1 components.

The total initial and final wave functions assumed are of the following form:

$$\begin{aligned}\Psi_{i(f)} = & \left|I_{i(f)};\ \tfrac{9}{2}+[624]\ (\tfrac{7}{2}-[514]);\ n=0\right\rangle \\ & + \sum_{\Omega_{i(f)},\alpha} \mu^{\alpha}_{i(f)} \left|I_{i(f)};\ \Omega_{i(f)}\,\alpha;\ 0\right\rangle \\ & + \sum_{\Omega_{f(i)},\alpha} \eta^{\alpha}_{i(f)} \left|I_{i(f)};\ \Omega_{f(i)}\,\alpha;\ 1\right\rangle\end{aligned} \qquad (2)$$

where n is the number of octupole phonons, the $\Omega\alpha$ represent the significant Nilsson single particle states $\Omega[Nn_z\Lambda]$, and the μ are the admixture coefficients for the Coriolis-mixed components. The coefficient η of the octupole vibration-particle mixing is given, for example, in the case of second-order mixing of the octupole band of the 7/2-[514] (ground) state into the initial 9/2+[624] band by:

$$\eta_i = -\frac{\hbar^2}{2\mathcal{J}} R' \frac{\langle I_i;\, \Omega_i = \frac{7}{2}+\alpha;\, n=0 | I_+ j_- | I_i;\, \Omega_i = \frac{9}{2}+[624];\, n=0\rangle}{\left(E_{\frac{9}{2}+[624]} - E_{\frac{7}{2}+\alpha}\right)}$$

$$\times \frac{R\langle I_i;\, \frac{7}{2}-[514];\, n=1 | H_{vp} | I_i;\, \Omega_i = \frac{7}{2}\alpha;\, n=0\rangle}{E_{\frac{9}{2}+[624]} - \left[E_{\frac{7}{2}-[514]} + E_3\right]} \qquad (3)$$

The pair reduction factors $R' = (U_1U_2 + V_1V_2)$, and $R = (U_1U_2 - V_1V_2)$ refer to the Coriolis and vibration-particle matrix elements, respectively. Normalization of the entire wave function is of course required.

Counting both collective and single-particle components a total of some 35 terms has been considered, of which perhaps 10 are of major significance. These terms include:

1). The principal and large Coriolis-mixed single-particle components which have small G(E1) values in the Nilsson model, e.g., 9/2+[624]→7/2-[514], 7/2+[633] →7/2-[514]; 2) Single-particle components arising from small Coriolis-mixed wave components but with large allowed G(E1) values by the Nilsson selection rules, e.g., 9/2+[624]→9/2-[514], 7/2+[624]→7/2-[514]; 3) The collective octupole E1 components arising from vibration-particle coupling; these terms dominate for the $\Delta K=0$ components. We are grateful to Profs. Aage Bohr and Ben Mottelson for calling our attention to the possible importance of the terms of type 2) above.

Since the relative phases of the collective E1 components are not known, we allowed that these be arbitrary. It was found that a single phase of the same

sign as the 7/2+[633] → 7/2-[514] single particle component gave the most satisfactory results.

In the microscopic calculations, we have allowed variation of only the single parameter $\langle a_3 \rangle$, the octupole amplitude. Pairing reduction factors have been calculated assuming λ, the chemical potential, to be at or near the energy $\tilde{\mathcal{E}}_j$ of the ground state 7/2-[514] Nilsson orbital. Ikegami and Udagawa[17] have shown that the pair reduction factors $(U_1U_2-V_1V_2)$ for electric multipole transitions can be estimated from empirical data on the basis of odd-even mass differences and the γ-ray transition energy. Their method is based upon the approximation $E_2 = \Delta$ which implies $\tilde{\mathcal{E}}_2 \cong \lambda$. Assuming this condition is met for the deformed nucleus ^{177}Hf, we have calculated the pair reduction factors R from experimental energy levels where known, and from the single-particle energies given in ref. 19) in all other cases. For the gap parameter Δ we have taken the value 0.60 MeV. The experimental odd-even mass difference P_n^{exp} is ~0.66 MeV for ^{177}Hf, but Δ is generally expected to be somewhat less than P_n^{exp}.[18] All calculations have assumed deformation $\eta = 5$ for ^{177}Hf. The pertinent Nilsson wave-function coefficients were obtained by a quadratic interpolation between $\eta = 2$, 4 and 6 using the Nilsson coefficients in ref. 20). The rotational constant $\hbar^2/2\mathfrak{J}$ has been taken from adjacent even-even nuclei as ~15.4 keV.

Table 2 shows the results of our calculations for ^{177}Hf, together with the values of B(E1) calculated using the simple 3-parameter fit described earlier. Absolute values of B(E1) obtained for the appropriate choice of $\langle a_3 \rangle$ in several cases of interest are displayed. Column 1 (NC) of the microscopic theory shows the results obtained when all assumptions

with regard to Coriolis mixing and pair reduction are taken into account and the calculations are performed within the Nilsson model, but no octupole mixing is assumed. There is clearly little relation between these results and experiment. Columns 2 and 3 (NCO and NCO') show the results for a similar calculation as column 1, but with inclusion of the octupole-particle coupling influence. In column 2 are given the results for the strict assumption $\lambda = \tilde{\varepsilon}_{7/2-[514]}$. This predicts $R_0 = 0.42$ for the principal single-particle component $9/2+[642] \rightarrow 7/2-[514]$. In order to give agreement with experiment for the highly hindered 321-keV E1, $\langle a_3 \rangle$ must be adjusted to 0.170. However, the apparent value R_0 indicated by the 3-parameter fit of data is ~0.34. In column 3 (NCO'), therefore, we show the results for $\lambda = 60$ keV above $\tilde{\varepsilon}_{7/2-[514]}$, $R_0 = 0.34$ and $\langle a_3 \rangle = 0.142$. Clearly, the calculated strength for the highly hindered 321-keV E1 is extremely sensitive to the choice of R_0 and to $\langle a_3 \rangle$. This sensitivity is a consequence of near cancellation between components opposite in phase. In general, however, the remaining transitions are much less sensitive to $\langle a_3 \rangle$, although the calculated branching ratios are rather easily upset. The values indicated for $\langle a_3 \rangle$ are in the range 0.1 - 0.2, consistent with the octupole amplitude expected in this region[13]. In column 4 we include a tabulation of results using pair reduction factors obtained by Vergnes and Rasmussen[2] from a solution of the BCS wave functions for N = 105. The agreement with experiment in this case, though still within an order of magnitude, is much poorer because the orbital energies $\tilde{\varepsilon}_{\Omega\alpha}$ differ somewhat from the best values for this particular nucleus and this BCS solution predicts $R_0 = 0.16$.

Finally, comment should be made concerning the apparently excellent quality of the fit that was obtained without use of Nilsson wave functions

simply by adjusting parameters which were assumed proportional to the three E1-matrix elements that contribute in first order Coriolis mixing. It can be easily shown that the effects on relative B(E1) values due to all first-order ($\Delta K=0$) corrections should be expressible by a single additional parameter if Coriolis mixing is treated only by first-order perturbation theory, without renormalizing wave functions. But the interference from $\Delta K = 0$ components is so large in this case that first-order perturbation treatment of the Coriolis interaction is inadequate. When normalized Coriolis-mixed wave functions from a full matrix diagonalization are used, however, the two-parameter theory no longer gives the linear plot in fig. 10, and much closer agreement with experiment is obtained. Moreover, the third parameter is now not redundant, and can give still better fits with experiment.

It is interesting in this regard to compare the values for the three parameters M_0, M_1 and M_2 used in the experimental fit with the various contributing terms calculated from theory involving the octupole vibration-particle mixing. The results of such a comparison are shown in table 3 for calculations assuming $\lambda \cong 60$ keV above $\tilde{\mathcal{E}}_{7/2-[514]}$ and $R_0 = 0.34$. Since the parameters M_0, M_1 and M_2 were adjusted to the strengths of the three E1's leading from the 9/2+[624] band head, the calculated values are shown as they apply to one particular transition, the 9/2+ → 9/2- 208 keV E1, for which all first order Coriolis-mixed components can contribute. The agreement is quite good for these low spin states, but for large spins the higher order Coriolis-mixed single-particle components complicate matters somewhat. In fact, in our calculations these small components are responsible for the increasing discrepancies between the theoretical and experimental values of B(E1) as high spins are

approached. It should also be noted that there are significant collective components arising from the particle transitions 5/2+[642] → 5/2-[512] and 5/2+[642] → 5/2-[523]. Because these contributions are nearly equal and opposite in phase, they are of consequence only for high spins. The quality of the 3-parameter fit for high spin states was thus apparently somewhat fortuitous, and resulted microscopically from a cancellation of several terms important for large values of the spin-dependent RPC matrix elements.

4. Conclusions

The general applicability of the interpretation of $|\Delta K| = 1$ E1 transitions in terms of Coriolis coupling, pairing, and vibration-particle coupling remains to be shown, but the results of our calculations for the nucleus ^{177}Hf indicate that the theoretical basis for the quantitative interpretation of E1 transitions in odd-mass deformed nuclei is established. More accurate knowledge of the pairing reduction factors and of the collective strengths B(E1) and B(E3) in odd-mass nuclei is essential to confirm the validity of our treatment. In the case of ^{177}Hf, direct experimental measurements of additional E1 lifetimes would be desirable, though present limitations in electronics make such measurements extremely difficult if not impossible.

5. Acknowledgements

We thank Dr. David Camp of Livermore for his assistance in obtaining spectra with the anti-Compton spectrometer, Mr. M. D. Holtz for making portions of his band-fit calculations available before publication and Dr. J. M. Hollander for many helpful discussions. We are also grateful to Profs. Aage Bohr and Ben Mottelson for their encouragement through stimulating discussions last summer.

This work was supported by the U. S. Atomic Energy Commission, partly through the Lawrence Radiation Laboratory and partly through an off-site contract on the University of California campus.

References

1) Yu. T. Grin and I. M. Pavlichenkov, Nucl. Phys. 65 (1965) 686

2) M. N. Vergnes and J. O. Rasmussen, Nucl. Phys. 62 (1965) 233

3) D. R. Nethaway and B. Mendoza, Lawrence Radiation Laboratory Report UCRL-70048 (1966)

4) A. J. Haverfield, F. M. Bernthal and J. M. Hollander, Nucl. Phys. A94 (1967) 337

5) P. Alexander, F. Boehm and E. Kankeleit, Phys. Rev. 133 (1964) B284

6) J. Blok and D. A. Shirley, Phys. Letters 13 (1964) 232

7) E. Bodenstedt, et al., Zeit. für Physik 190 (1966) 60

8) E. E. Berlovich, Yu. K. Gusev, V. V. Il'in and M. K. Nikitin, Soviet Physics JETP 43 (1962) 1625

9) H. I. West, Jr., L. G. Mann and R. J. Nagle, Phys. Rev. 124 (1961) 527

10) B. Elbek, M. C. Olesen and O. Skilbreid, Nucl. Phys. 10 (1959) 294

11) M. D. Holtz, private communication

12) V. G. Soloviev, JINR P-1973 (1966)

13) W. Donner and W. Greiner, Zeit. für Physik 197 (1966) 440

14) A. Faessler and A. Plastino, University of California, Los Angeles, preprint (1967)

15) G. Monsonego and R. Piepenbring, Nucl. Phys. 78 (1966) 265

16) A. Faessler, T. Udagawa and R. K. Sheline, Nucl. Phys. 85 (1966) 670

17) H. Ikegami and T. Udagawa, Phys. Rev. 133 B (1964) 1388

18) S. G. Nilsson and O. Prior, Kgl. Danske Videnskab. Selskab, Mat. Fys. Medd. 32 No. 16 (1961). cf. also J. O. Rasmussen and C. W. Ma, Zeitschrift für Physik (in press).

19) C. Gustafson, I. L. Lamm, B. Nilsson and S. G. Nilsson, preprint, Lund Inst. Tech. (1966)

20) S. G. Nilsson, Kgl. Danske Videnskab. Selskab, Mat. Fys. Medd. 29, No. 16 (1954)

Table 1. Experimental relative intensities and derived reduced transition strengths for ^{177}Hf E1's

initial spin	final spin	E_γ (keV)	intensity[a]	B(E1) (MeV-fm^3)×10^5
9/2	7/2	321.3	8.8(5)	0.034(4)
9/2	9/2	208.3	524(21)	9.2(6)
9/2	11/2	71.7	7.2(4)	3.1(2)
11/2	9/2	313.7	10.0(5)	0.66(5)
11/2	11/2	177.0	27.8(1.2)	10.3(7)
11/2	13/2	(17.2)		
13/2	11/2	305.5	14.2(6)	2.32(13)
13/2	13/2	145.8	7.7(5)	11.6(9)
15/2	13/2	299.0	12.6(7)	4.3(3)
15/2	15/2	117.2	2.0(2)	11.5(1.3)
17/2	15/2	291.4	8.4(8)	7.0(7)
17/2	17/2	88.4	0.32(8)	9.4(2.4)
19/2	17/2	292.5	6.7(7)	8.9(9)
19/2	19/2	69.2	0.088(30)	8.6(2.9)
21/2	19/2	283.4	2.9(5)	11.0(2.0)
21/2	21/2	(41.0)		

[a]Normalized to 105.4-keV γ ray = 100. For most Ge(Li) detectors with thicker windows than ours, this is an unfortunate choice for normalization, since 105 keV does not fall in the near-exponential region of the efficiency curve. This may account for part of the discrepancy between our measured intensities for the strong lines and those quoted in ref. 4. In general, we measure I_γ about 10% greater than ref. 4 for those strong lines > 200 keV in energy.

Table 2. Theoretical values of B(E1) for ^{177}Hf

initial spin K=9/2+	final spin K=7/2-	reduced strength B(E1) (MeV-fm^3)×10^5 3-parameter fit	microscopic theory NC[a]	NCO[b]	NCO'[c]	NCOBCS[d]	experiment
9/2	7/2	0.034	3.4	0.031	0.038	0.034	0.034(4)
9/2	9/2	7.5	0.74	10.0	6.3	2.4	9.2(6)
9/2	11/2	3.5	0.05	6.5	3.9	1.6	3.1(2)
11/2	9/2	0.69	2.1	0.69	0.42	0.70	0.66(5)
11/2	11/2	9.7	0.87	12.4	7.8	2.9	10.3(7)
11/2	13/2	7.6	0.06	11.5	6.9	3.1	
13/2	11/2	2.6	1.3	3.5	2.3	2.3	2.32(13)
13/2	13/2	10.1	0.77	11.9	7.4	2.8	11.6(9)
15/2	13/2	5.0	0.74	7.0	4.6	4.4	4.3(3)
15/2	15/2	9.7	0.59	10.4	6.4	2.3	11.5(1.3)
17/2	15/2	7.3	0.34	10.7	7.2	6.8	7.0(7)
17/2	17/2	8.9	0.40	8.6	5.2	1.9	9.4(2.4)
19/2	17/2	8.2	0.14	13.6	9.2	9.1	8.9(9)
19/2	19/2	7.9	0.24	6.8	4.0	1.4	8.6(2.9)
21/2	19/2	11.0	0.01	16.3	11.2	11.8	11.0(2.0)
21/2	21/2	6.9	0.10	5.1	2.9	0.93	

[a] Assumes $\lambda=\tilde{\varepsilon}_{7/2-[514]}$, $\langle\alpha_3\rangle=0$, and $R_0=(U_{9/2+[624]}U_{7/2-[514]}-V_{9/2+[624]}V_{7/2-[514]})=0.42$

[b] $\lambda=\tilde{\varepsilon}_{7/2-[514]}$, $\langle\alpha_3\rangle=0.170$, $R_0=0.42$

[c] $\lambda=\tilde{\varepsilon}_{7/2-[514]}+60$ keV, $\langle\alpha_3\rangle=0.142$, $R_0=0.34$

[d] $\lambda=\tilde{\varepsilon}_{7/2-[514]}+70$ keV, BCS solution, $\langle\alpha_3\rangle=0.142$, $R_0=0.16$

Table 3. Calculated contributions to the experimental parameters M_0, M_1, and M_2 (for the I_i=9/2, I_f=9/2 transition)

initial band	final band	octupole phonons n_i	n_f	mixing coeff. product[a]	$(U_iU_f-V_iV_f)$	E1 matrix element[b]	product
9/2+[624]	7/2-[514]	0	0	0.96	0.34	1.7×10^{-2}	5.5×10^{-3}
						Experimental $M_0=5.5\times10^{-3}$	
7/2+[633]	7/2-[514]	0	0	0.25	-0.57	-8.3×10^{-3}	1.2×10^{-3}
"	"	1	0	-5.1×10^{-2}		-7.3×10^{-2}	3.7×10^{-3}
"	"	0	1	-8.9×10^{-2}		-7.3×10^{-2}	6.5×10^{-3}
7/2+[624]	"	0	0	-4.4×10^{-3}	0.64	0.56	-1.6×10^{-3}
"	"	1	0	1.7×10^{-3}		-7.3×10^{-2}	-1.2×10^{-4}
"	"	0	1	3.0×10^{-3}		-7.3×10^{-2}	-2.2×10^{-4}
7/2+[613]	"	0	0	6.4×10^{-3}	0.64	6.2×10^{-2}	2.5×10^{-4}
"	"	1	0	8.8×10^{-4}		-7.3×10^{-2}	-6.4×10^{-5}
"	"	0	1	1.5×10^{-3}		-7.3×10^{-2}	-1.0×10^{-4}
							Sum=0.96×10^{-2}
				Experimental $\sqrt{I_i(I_i-1)-K_i(K_i-1)}\ M_1 = 3\times M_1=1.0\times10^{-2}$			
9/2+[624]	9/2-[505]	0	0	6.3×10^{-2}	0.87	-3.4×10^{-3}	-1.9×10^{-4}
"	"	1	0	7.5×10^{-3}		-7.3×10^{-2}	-5.5×10^{-4}
"	"	0	1	1.3×10^{-2}		-7.3×10^{-2}	-9.5×10^{-4}
"	9/2-[514]	0	0	-3.5×10^{-3}	-0.31	0.54	5.9×10^{-4}
"	"	1	0	-7.9×10^{-4}		-7.3×10^{-2}	5.8×10^{-5}
"	"	0	1	-1.4×10^{-3}		-7.3×10^{-2}	1.0×10^{-4}
							Sum = -0.94×10^{-3}
				Experimental $\sqrt{I_f(I_f+1)-K_f(K_f+1)}\ M_2=3\times M_2=-1.3\times10^{-3}$			

[a] Represents the wave function coefficient product for the indicated initial and final particle or particle-phonon states.

[b] For particle components, $\sqrt{3/4\pi}\ e_{eff}(\hbar/M\omega_0)^{1/2}G(E1)$; for collective components, derived from eq. (1). We have assumed e_{eff} = (Ze/A).

Figure Captions

Fig. 1. The γ-ray spectrum of $^{177}Lu^m$ in the region 170-250 keV showing the location of the 242.5-keV cascade transition

Fig. 2. Linear plot of the 88.4-keV E1 γ ray from an anti-Compton spectrum of $^{177}Lu^m$ decay. (Scale: ~0.080 keV/channel)

Fig. 3. Linear plot of the 242.5-keV γ ray from $^{177}Lu^m$ decay. (Scale: 0.080 keV/channel)

Fig. 4. Linear plot of the 69.2-keV E1 γ ray from $^{177}Lu^m$ decay. (Scale: 0.038 keV/channel)

Fig. 5. High resolution γ-ray spectrum of $^{177}Lu^m$ in the region 100-150 keV

Fig. 6. High resolution γ-ray spectrum of $^{177}Lu^m$ in the region 275-330 keV

Fig. 7. The decay scheme of $^{177}Lu^m$ from ref. 5 with additions from refs. 4, 6, 7, and the present work

Fig. 8. Plot of the M1-E2 branching ratio for cascade transitions in the $K = 9/2+$ band of ^{177}Hf. Derived from crossover-to-cascade ratios of γ ray intensities from decay of $^{177}Lu^m$

Fig. 9. Diagram of the E1 branching ratios in ^{177}Hf from the data in Table 1 and the simple 2-parameter theory of refs. 1 and 2

Fig. 10. The normalized 3-parameter fit of absolute reduced E1 strengths in ^{177}Hf for the $\Delta I = -1$ class of transition. Derived from the form $B(E1) = [M_o(I_i\ 1\ 9/2\ -1|I_f\ 7/2) + M_1\sqrt{I_i(I_i+1)-(9/2)(7/2)}\ (I_i\ 1\ 7/2\ 0|I_f\ 7/2) + M_2\sqrt{I_f(I_f+1)-(7/2)(9/2)}\ (I_i\ 1\ 9/2\ 0|I_f\ 9/2)]^2$ with $M_o = 5.5 \times 10^{-3}$, $M_1 = 3.4 \times 10^{-3}$, and $M_2 = -4.5 \times 10^{-4}$

Fig. 11. Normalized 3-parameter fit of the reduced E1 strengths in ^{177}Hf for the $\Delta I = 0$ class of transition

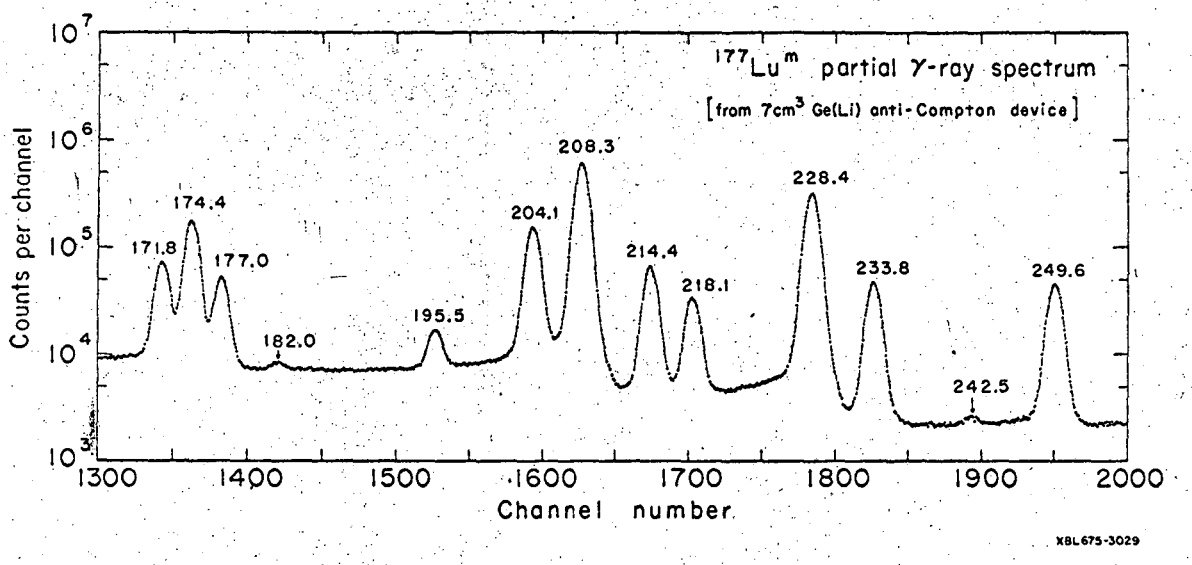
$^{177}Lu^{m}$ partial γ-ray spectrum
[from 7cm³ Ge(Li) anti-Compton device]
Counts per channel
Channel number
171.8
174.4
177.0
182.0
195.5
204.1
208.3
214.4
218.1
228.4
233.8
242.5
249.6
XBL675-3029

Fig. 1

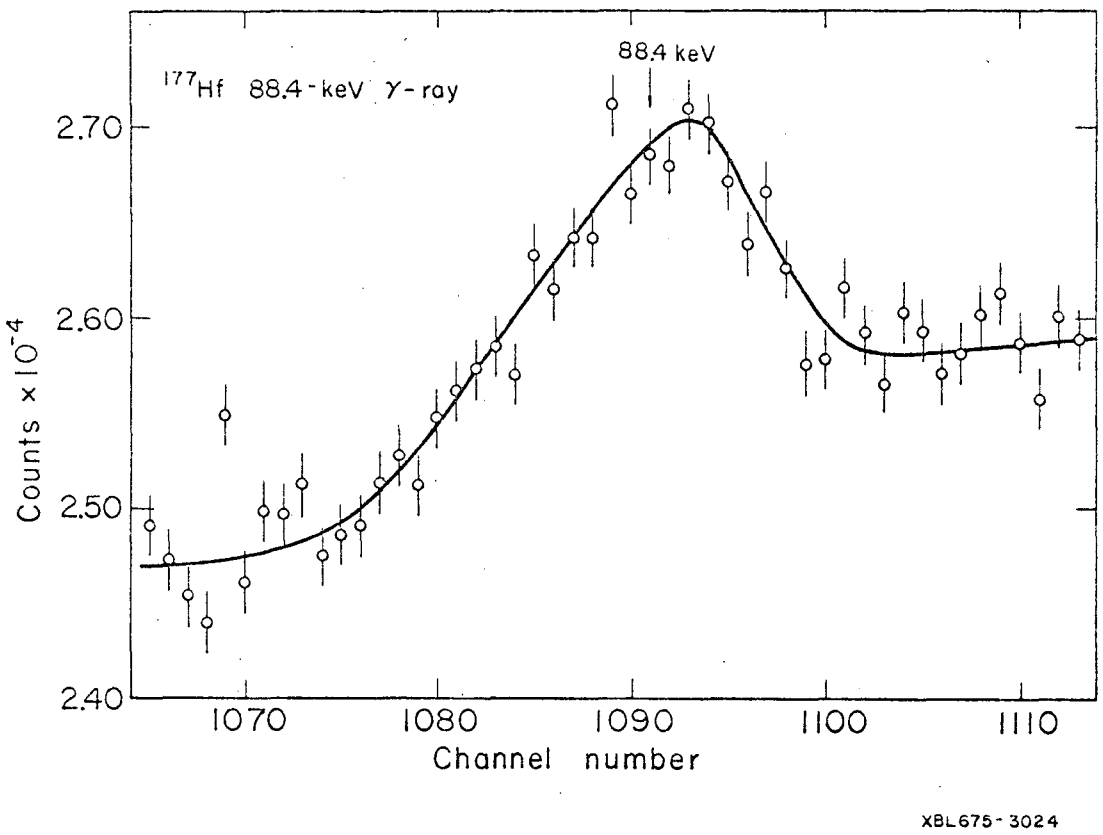
^{177}Hf 88.4-keV γ-ray
88.4 keV
2.70
2.60
2.50
2.40
Counts × 10^{-4}
1070
1080
1090
1100
1110
Channel number
XBL675-3024

Fig. 2

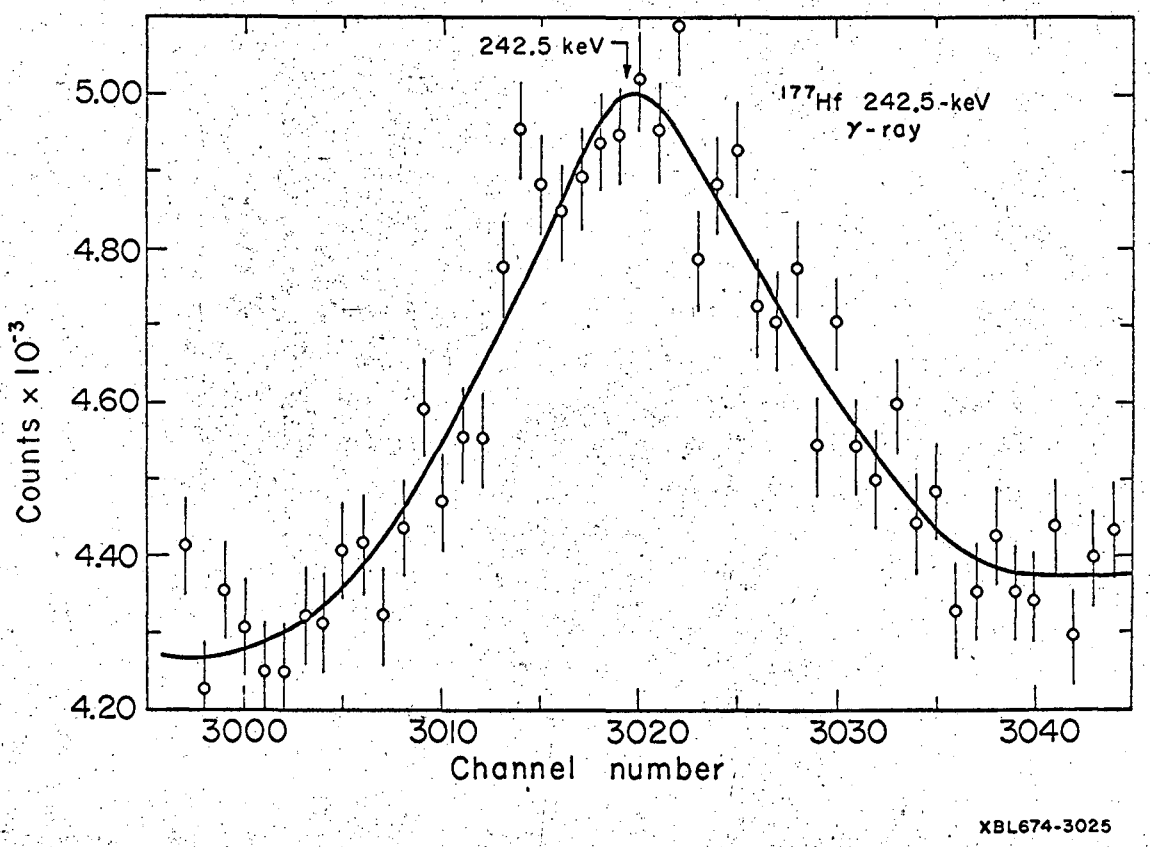
242.5 keV
^{177}Hf 242.5-keV
γ-ray
5.00
4.80
4.60
4.40
4.20
Counts × 10^{-3}
3000
3010
3020
3030
3040
Channel number
XBL674-3025

Fig. 3

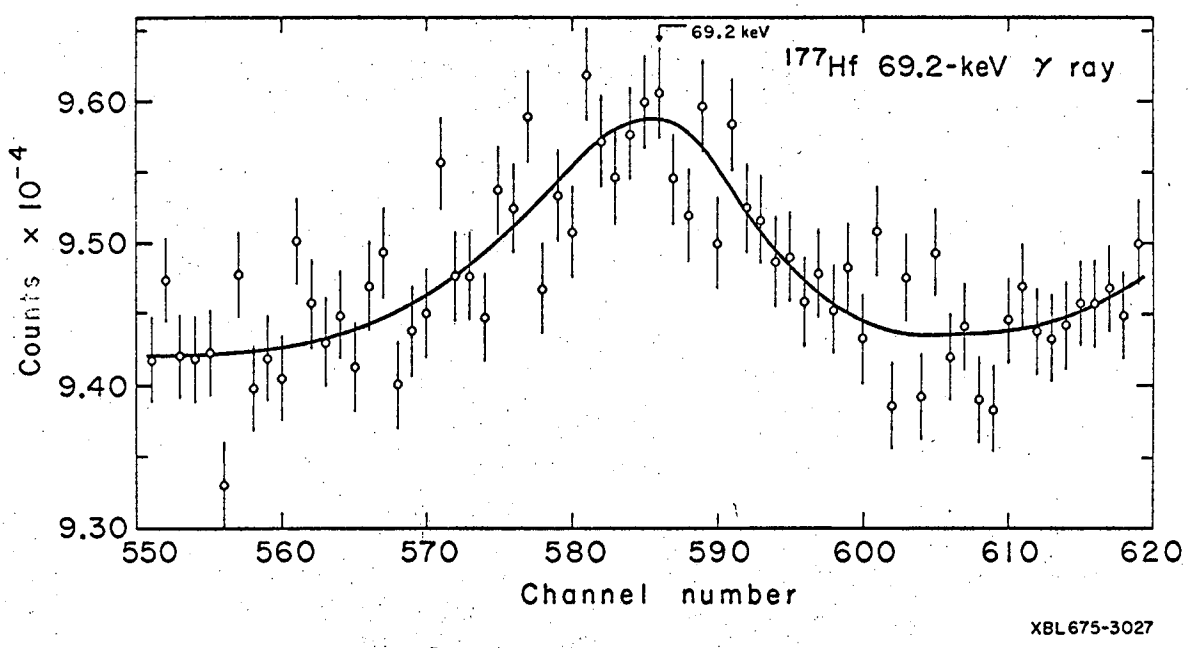
69.2 keV
^{177}Hf 69.2-keV γ ray
Counts × 10^{-4}
9.60
9.50
9.40
9.30
550
560
570
580
590
600
610
620
Channel number
XBL675-3027

Fig. 4

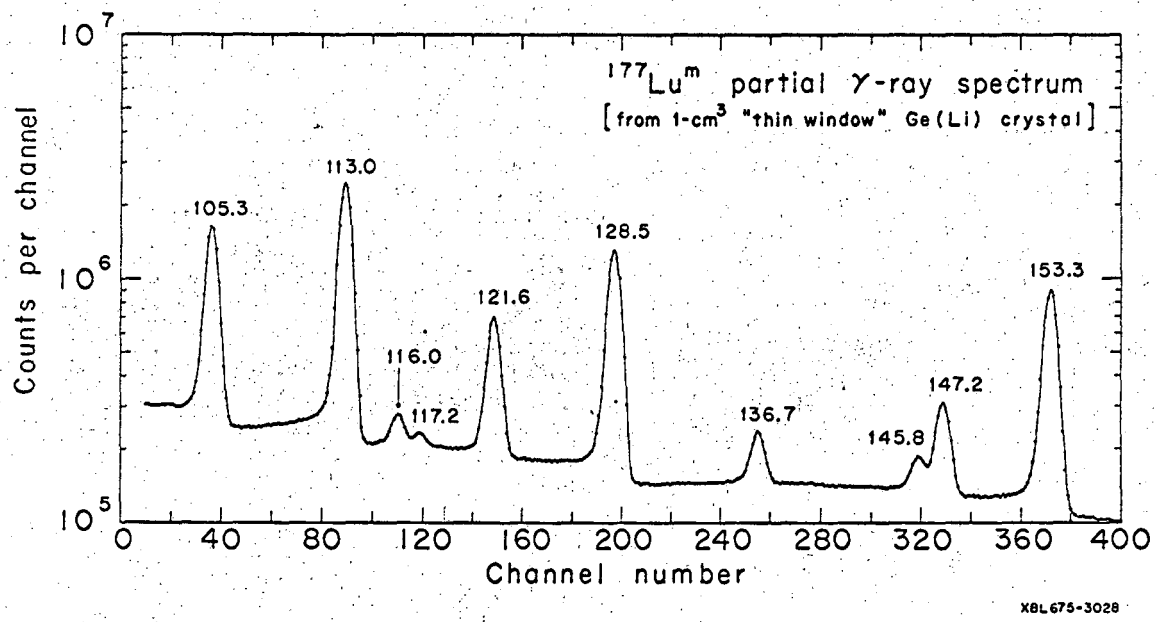
$^{177}Lu^{m}$ partial γ-ray spectrum
[from 1-cm³ "thin window" Ge(Li) crystal]
105.3
113.0
116.0
117.2
121.6
128.5
136.7
145.8
147.2
153.3
Counts per channel
Channel number
10^7
10^6
10^5
0
40
80
120
160
200
240
280
320
360
400
XBL675-3028

Fig. 5

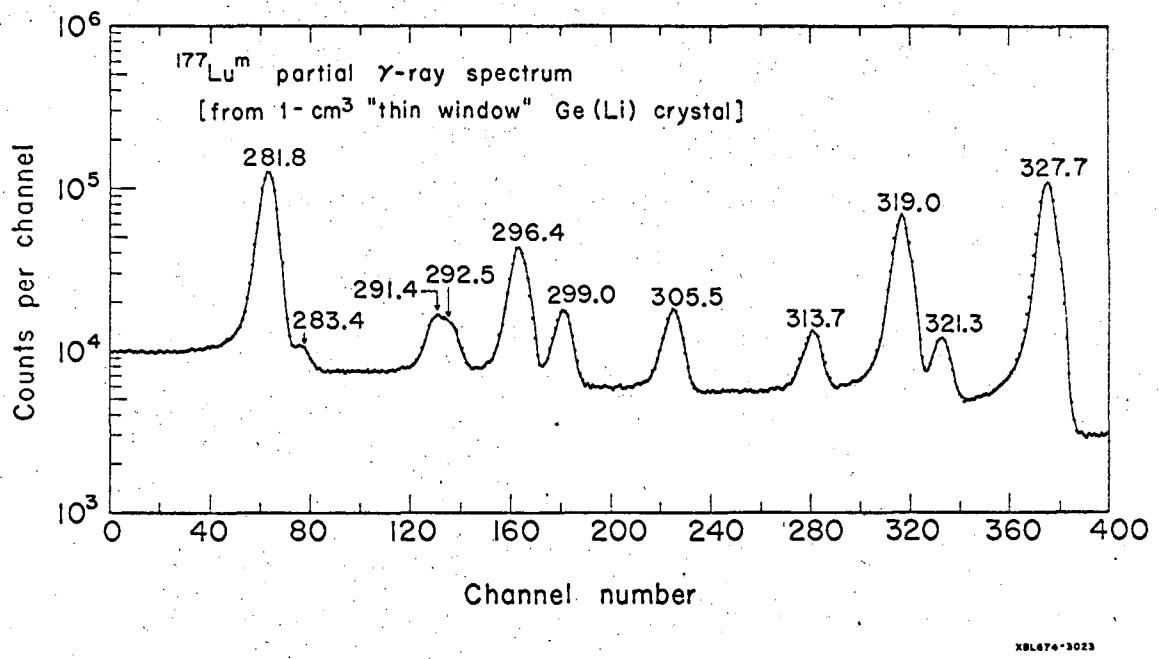
$^{177}Lu^{m}$ partial γ-ray spectrum
[from 1-cm³ "thin window" Ge(Li) crystal]
281.8
283.4
291.4
292.5
296.4
299.0
305.5
313.7
319.0
321.3
327.7
Counts per channel
Channel number
XBL674-3023

Fig. 6

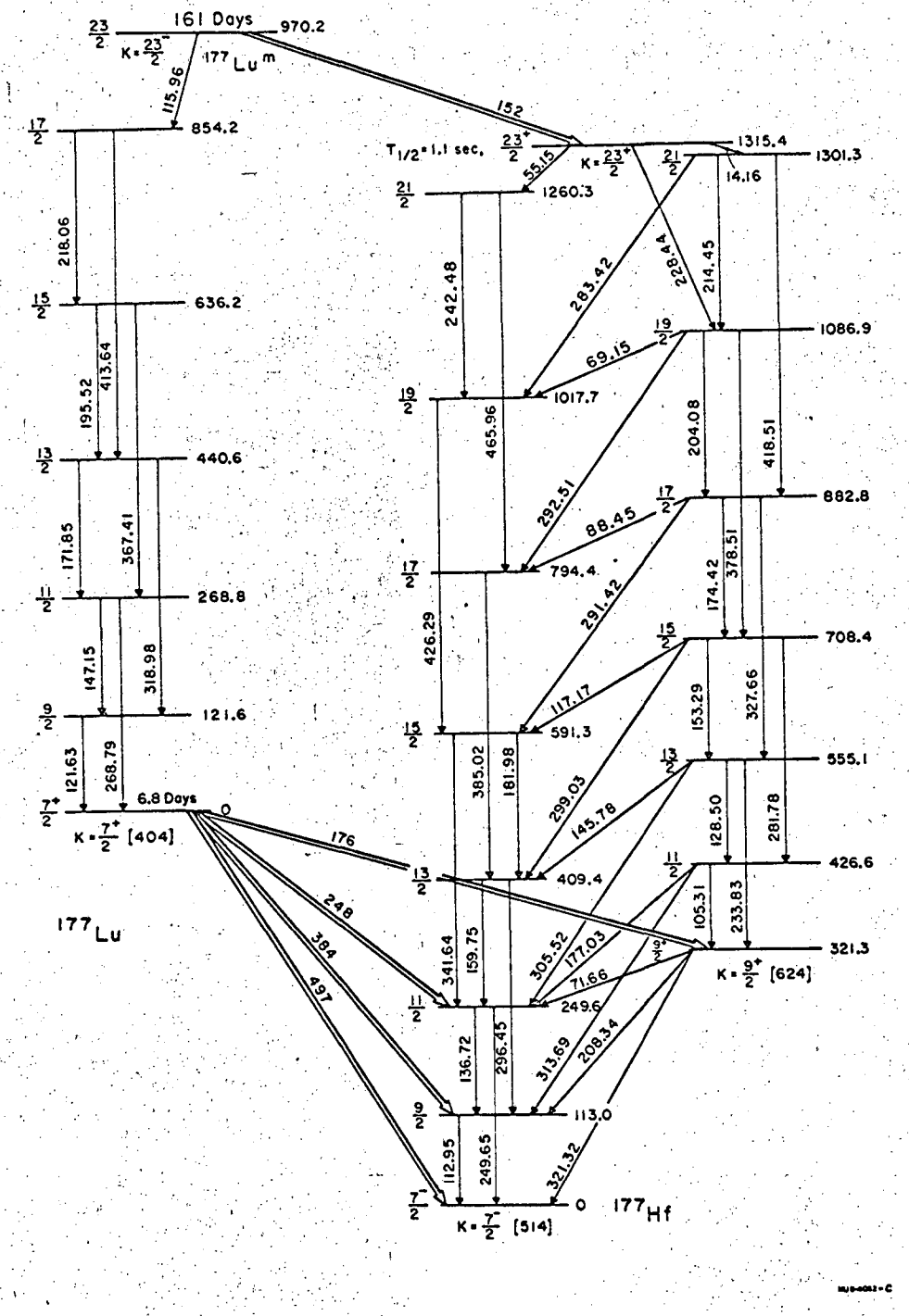
161 Days
970.2
K = 23/2⁻
177 Lu m
115.96
152
854.2
636.2
440.6
268.8
121.6
6.8 Days
K = 7/2⁺ [404]
177 Lu
T1/2 = 1.1 sec.
K = 23/2⁺
1315.4
1301.3
1260.3
1086.9
1017.7
882.8
794.4
708.4
591.3
555.1
409.4
426.6
321.3
K = 9/2⁺ [624]
249.6
113.0
0
177 Hf
K = 7/2⁻ [514]
218.06
195.52
413.64
171.85
367.41
147.15
318.98
121.63
268.79
176
248
384
497
55.15
14.16
242.48
283.42
228.4
214.45
69.15
465.96
204.08
418.51
292.51
88.45
174.42
378.51
291.42
426.29
117.17
153.29
327.66
385.02
181.98
299.03
145.78
128.50
281.78
105.31
233.83
341.64
159.75
305.52
177.03
71.66
136.72
296.45
313.69
208.34
112.95
249.65
321.32

Fig. 7

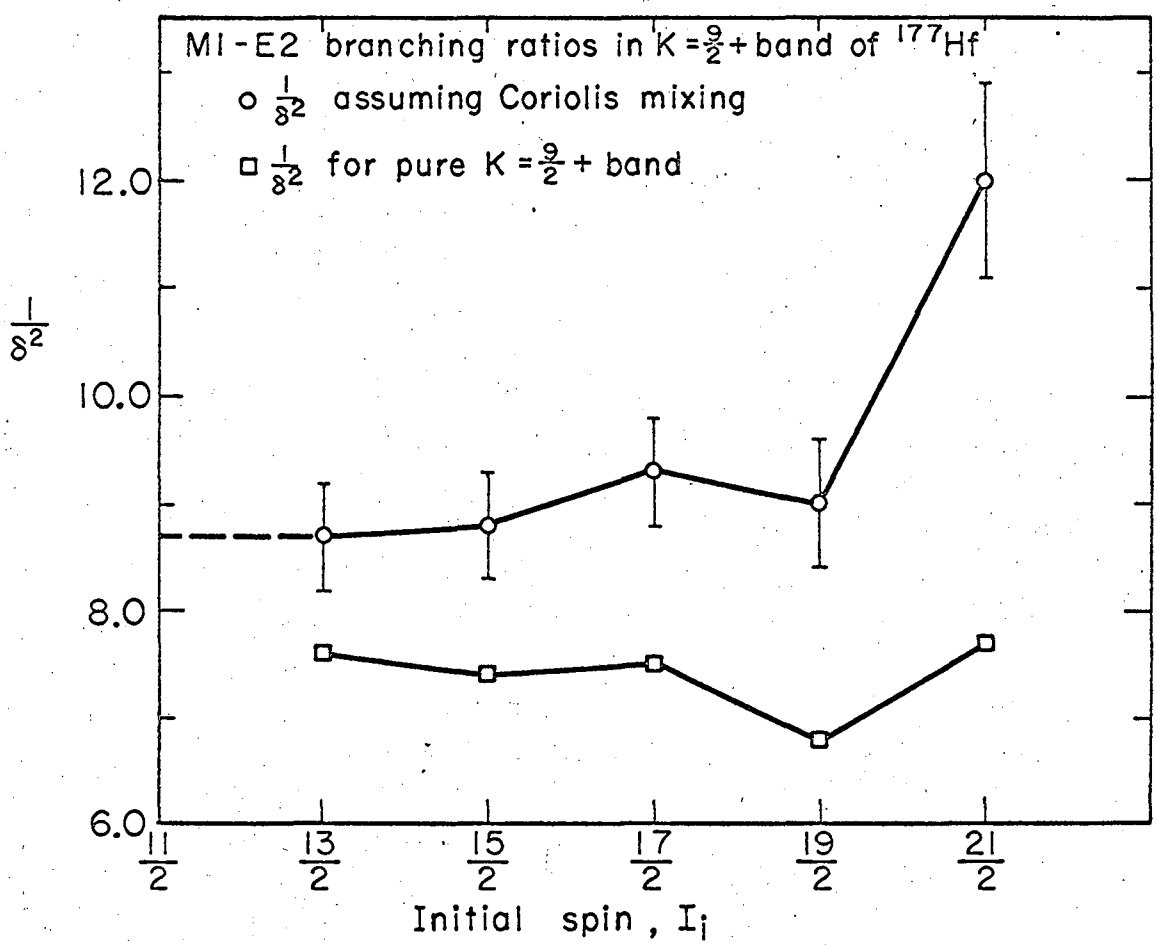

XBL675-3026

Fig. 8

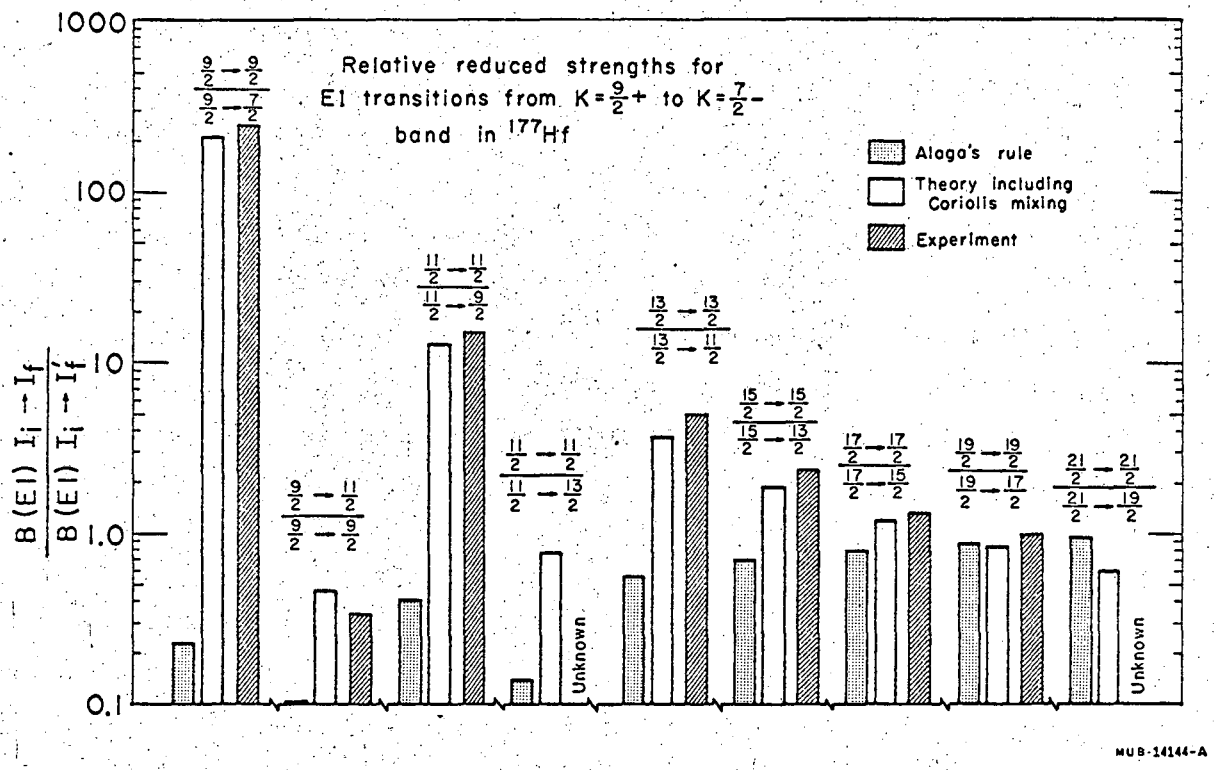
Relative reduced strengths for
E1 transitions from K=9/2+ to K=7/2-
band in 177Hf
Alaga's rule
Theory including Coriolis mixing
Experiment
1000
100
10
1.0
0.1
B(E1) Ii → If / B(E1) Ii → I'f
9/2 → 9/2 / 9/2 → 7/2
9/2 → 11/2 / 9/2 → 9/2
11/2 → 11/2 / 11/2 → 9/2
11/2 → 11/2 / 11/2 → 13/2
Unknown
13/2 → 13/2 / 13/2 → 11/2
15/2 → 15/2 / 15/2 → 13/2
17/2 → 17/2 / 17/2 → 15/2
19/2 → 19/2 / 19/2 → 17/2
21/2 → 21/2 / 21/2 → 19/2
Unknown
MUB-14144-A

Fig. 9

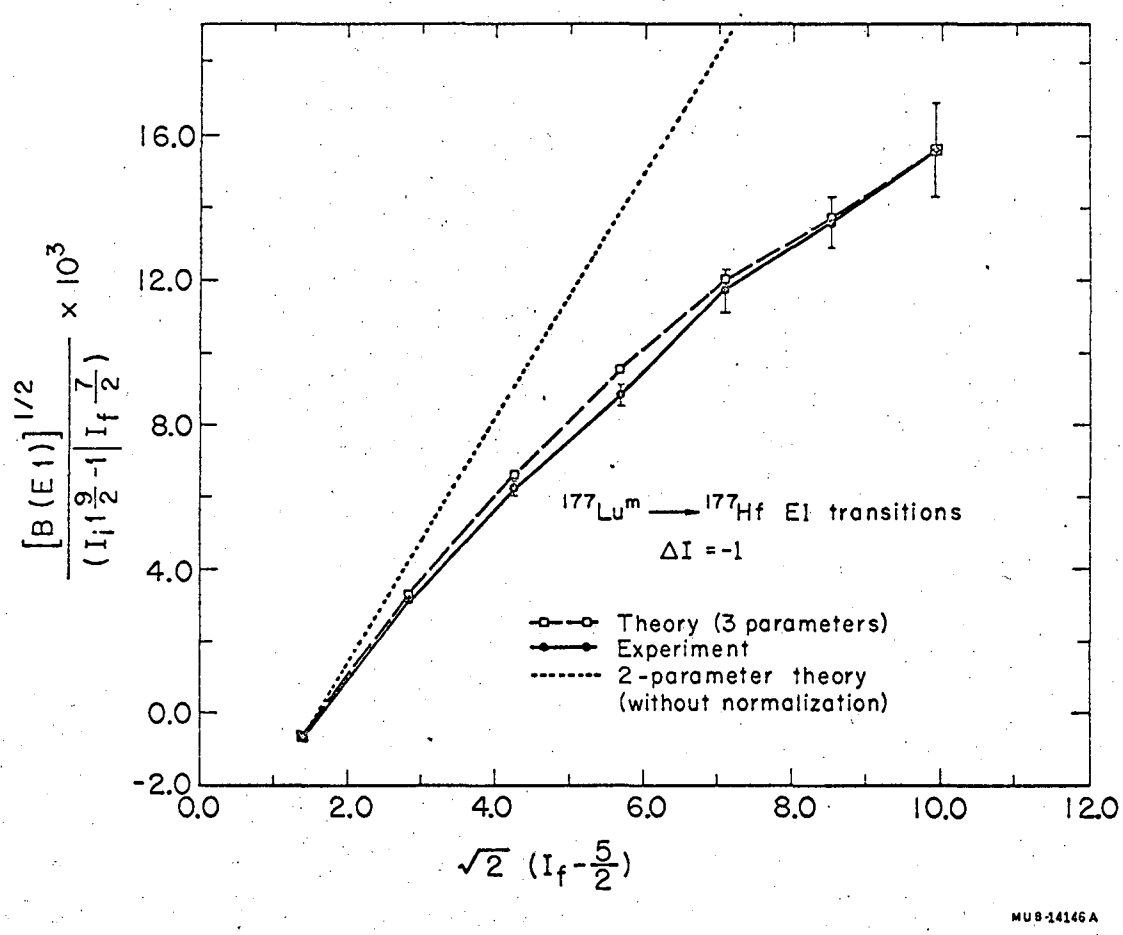
16.0
12.0
8.0
4.0
0.0
-2.0
0.0
2.0
4.0
6.0
8.0
10.0
12.0
$\frac{[B(E1)]^{1/2}}{(I_i 1 \frac{9}{2} -1 | I_f \frac{7}{2})} \times 10^3$
$\sqrt{2}\ (I_f - \frac{5}{2})$
$^{177}Lu^m \longrightarrow {}^{177}Hf$ E1 transitions
$\Delta I = -1$
Theory (3 parameters)
Experiment
2-parameter theory
(without normalization)
MU8-14146A

Fig. 10

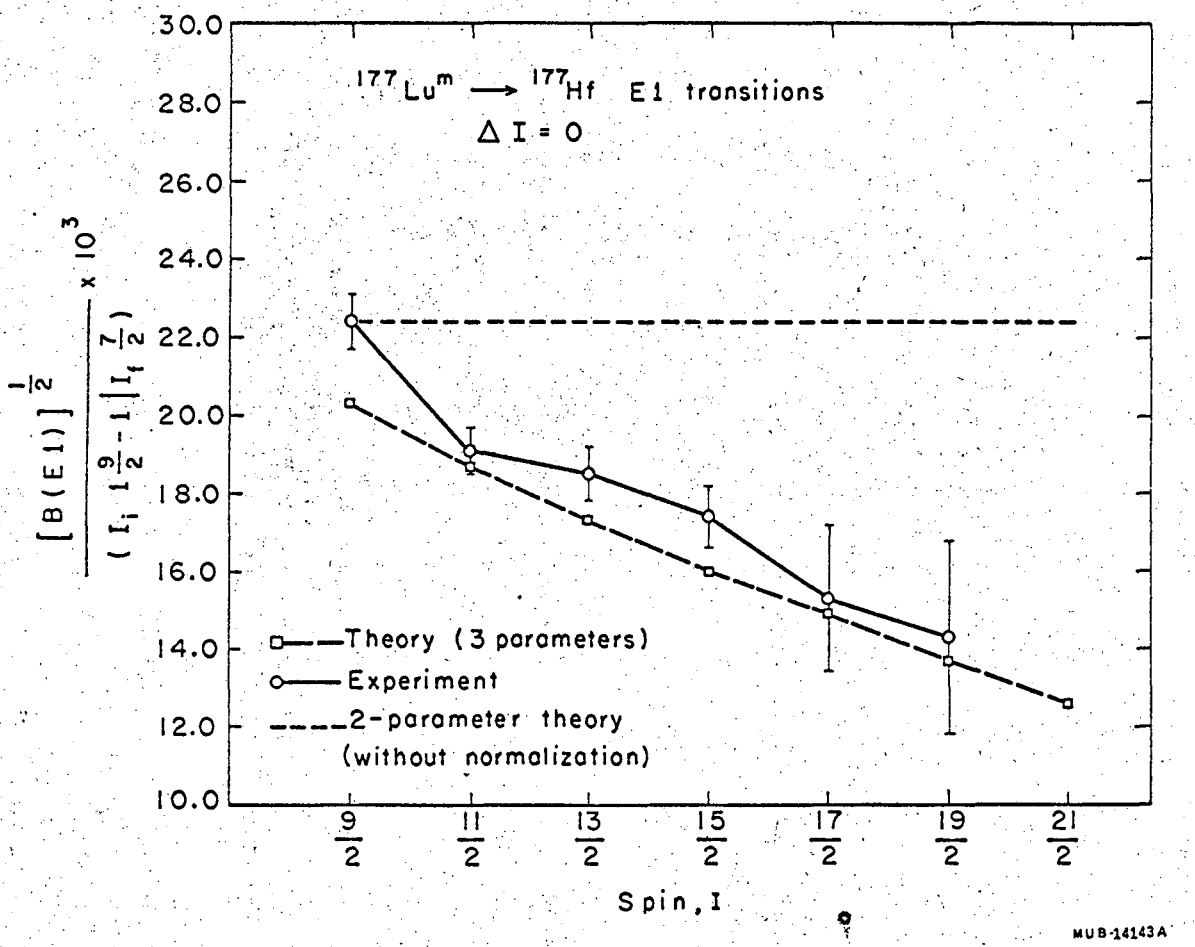

$^{177}Lu^m \longrightarrow {}^{177}Hf$ E1 transitions
$\Delta I = 0$
$\frac{[B(E1)]^{\frac{1}{2}}}{(I_i\, 1\frac{9}{2}-1 | I_f\, \frac{7}{2})} \times 10^3$
30.0
28.0
26.0
24.0
22.0
20.0
18.0
16.0
14.0
12.0
10.0
Theory (3 parameters)
Experiment
2-parameter theory
(without normalization)
9/2
11/2
13/2
15/2
17/2
19/2
21/2
Spin, I
MUB-14143A

Fig. 11

This report was prepared as an account of Government sponsored work. Neither the United States, nor the Commission, nor any person acting on behalf of the Commission:

A. Makes any warranty or representation, expressed or implied, with respect to the accuracy, completeness, or usefulness of the information contained in this report, or that the use of any information, apparatus, method, or process disclosed in this report may not infringe privately owned rights; or

B. Assumes any liabilities with respect to the use of, or for damages resulting from the use of any information, apparatus, method, or process disclosed in this report.

As used in the above, "person acting on behalf of the Commission" includes any employee or contractor of the Commission, or employee of such contractor, to the extent that such employee or contractor of the Commission, or employee of such contractor prepares, disseminates, or provides access to, any information pursuant to his employment or contract with the Commission, or his employment with such contractor.